Chapter 5 | Air Temperature and Humidity in the PBL

5.1 Factors Influencing Air Temperature and Humidity

The following factors and processes influence the vertical distribution (profile) of air temperature in the atmospheric boundary layer.

- Type of air mass and its temperature just above the PBL, which depend on the synoptic situation and the large-scale circulation pattern.
- Thermal characteristics of the surface and submedium, which influence the diurnal range of surface temperatures.
- Net radiation at the surface and its variation with height, which determine the radiative warming or cooling of the surface and the PBL.
- Sensible heat flux at the surface and its variation with height, which determine the rate of warming or cooling of the air due to convergence or divergence of sensible heat flux.
- Latent heat exchanges during evaporation and condensation processes at the surface and in air, which influence the surface and air temperatures, respectively.
- Warm or cold air advection as a function of height in the PBL.
- Height or the PBL to which turbulent exchanges of heat are confined.

Similarly, the factors influencing the specific humidity or mixing ratio of water vapor in the PBL are as follows:

- Specific humidity of air mass just above the PBL.
- Type of surface, its temperature, and availability of moisture for evaporation and/or transpiration.
- The rate of evapotranspiration or condensation at the surface and the variation of water vapor flux with height in the PBL.
- Horizontal advection of water vapor as a function of height.
- Mean vertical motion in the PBL and possible cloud formation and precipitation processes.
- The PBL depth through which water vapor is mixed.

The vertical exchanges of heat and water vapor are primarily through turbulent motions in the PBL; the molecular exchanges are important only in a very thin (of the order of 1 mm or less) layer adjacent to the surface. In the atmospheric PBL, turbulence is generated mechanically (due to surface friction and wind shear) and/or convectively (due to surface heating and buoyancy). These two types of turbulent motions are called forced convection and free convection, respectively. The combination of the two is sometimes referred to as mixed convection, although more often the designation 'forced' or 'free' is used, depending on whether a mechanical or convective exchange process dominates.

The convergence or divergence of sensible heat flux leads to warming or cooling of air, similar to that due to net radiative flux divergence or convergence. The rate of warming is equal to the vertical gradient of $-H/\rho c_p$, i.e., $\partial T/\partial t = -(\partial H/\partial z)/\rho c_p$. Thus a gradient of 1 W m^{-3} in sensible heat flux will produce a change in air temperature at the rate of about $3°C$ h^{-1}. Similarly, divergence or convergence of water vapor flux leads to decrease or increase of specific humidity with time.

Horizontal advections of heat and moisture become important only when there are sharp changes in the surface characteristics (e.g., during the passage of a front) in the horizontal. Mean vertical motions forced by changes in topography often lead to rapid changes in temperature and humidity of air, as well as to local cloud formation and precipitation processes, as moist air rises over the mountain slopes. Equally sharp changes occur on the lee sides of mountains. Even over a relatively flat terrain, the subsidence motion often leads to considerable warming and drying of the air in the PBL.

5.2 Basic Thermodynamic Relations and the Energy Equation

The pressure in the lower atmosphere decreases with height in accordance with the hydrostatic equation

$$\partial P/\partial z = -\rho g \tag{5.1}$$

Equation (5.1) is strictly valid only for the atmosphere at rest. It is also a good approximation for large-scale atmospheric flows. For small mesoscale and microscale motions, however, the deviations from the hydrostatic equation due to vertical motions and accelerations may also become significant. But, in thermodynamical relations discussed here, the atmosphere is assumed to be in a hydrostatic equilibrium.

Another fundamental relationship between the commonly used thermodynamic variables is the equation of state or the ideal gas law

$$P = R\rho T = (R_*/m)\rho T \tag{5.2}$$

in which R is the specific gas constant, $R_* = 8.314$ J K^{-1} mole^{-1} is the absolute gas constant, and m is the mean molecular mass of air.

Some of the thermodynamic relations follow from the first law of thermodynamics which is essentially a statement about the conservation of energy. When applied to an air parcel, the law states that an increase in the internal energy, dU, of the parcel can occur only through an addition of heat, dH, to the parcel and/or by performing work, dW, on the parcel. This can be expressed mathematically as

$$dU = dH + dW \qquad (5.3a)$$

where each term may be considered to represent unit volume of the parcel.

Experimental evidence suggests that the internal energy per unit volume of an ideal gas is proportional to its absolute temperature, so that $dU = \rho c_p\, dT$ for a constant pressure process, and $dU = \rho c_v\, dT$ for a constant volume process. Here, c_p and c_v are the specific heat capacities at constant pressure and volume, respectively. Their difference is equal to the specific gas constant, that is $c_p - c_v = R$ (for dry air, $c_p = 1005$ J K^{-1} kg^{-1} and $R = 287.04$ J K^{-1} kg^{-1}).

Expressing the work done on the air parcel in terms of pressure and volume, one can derive several different expressions of the first law of thermodynamics (Hess, 1959; Fleagle and Businger, 1980). Here, we give only the one involving changes in temperature and pressure

$$\rho c_p dT = dH + dP \qquad (5.3b)$$

which implies that the parcel temperature may change due to an addition of heat and/or a change in pressure.

If a parcel of air is lifted upward in the atmosphere, its pressure will decrease in response to decreasing pressure of its surroundings. This will lead to a decrease in the temperature and, possibly, to a decrease in the density of the parcel (due to expansion of the parcel) in accordance with Equation (5.2). If there is no exchange of heat between the parcel and the surrounding environment, the above process is called adiabatic. Vertical turbulent motions in the PBL, which carry air parcels up and down, are rapid enough to justify the assumption that changes in thermodynamic properties of such parcels are adiabatic ($dH = 0$). The rate of change of temperature of such a parcel with height can be calculated from Equations (5.1) and (5.3b) and is characterized by the adiabatic lapse rate (Γ)

$$\Gamma = -(\partial T/\partial z)_{ad} = g/c_p \qquad (5.4)$$

This is also the temperature lapse rate (rate of decrease of temperature with height) in an adiabatic atmosphere, which under dry or unsaturated conditions amounts to 0.0098 K m^{-1} or nearly 10 K km^{-1}.

The relationship between the changes of temperature and pressure in a parcel moving adiabatically, as well as those in an adiabatic atmosphere, are also given by Equations (5.2) and (5.3b), with $dH = 0$:

$$dT/T = (R/c_p)(dP/P) \qquad (5.5)$$

integration of which gives the Poisson equation

$$T = T_0(P/P_0)^k \qquad (5.6)$$

where T_0 is the temperature corresponding to the reference pressure P_0 and the exponent $k = R/c_p \cong 0.286$.

Equation (5.6) is used to relate the potential temperature Θ, defined as the temperature which an air parcel would have if it were brought down to a pressure of 1000 mbar adiabatically from its initial state, to the actual temperature T as

$$\Theta = T(1000/P)^k \qquad (5.7)$$

where P is in millibars. The potential temperature has the convenient property of being conserved during vertical movements of an air parcel, provided heat is not added or removed during such excursions. Then, the parcel may be identified or labeled by its potential temperature. In an adiabatic atmosphere, potential temperature remains constant with height. For a nonadiabatic or diabatic atmosphere, it is easy to show from Equation (5.7) that, to a good approximation,

$$\frac{\partial \Theta}{\partial z} = \frac{\Theta}{T}\left(\frac{\partial T}{\partial z} + \Gamma\right) \cong \frac{\partial T}{\partial z} + \Gamma \qquad (5.8)$$

This approximation is particularly useful in the PBL where potential and actual temperatures, in absolute units, do not usually differ by more than 10%. The above relationship is often used to express the difference in the potential temperatures between any two height levels as

$$\Delta\Theta = \Delta T + \Gamma\Delta z \qquad (5.9)$$

An integral version of the same relationship,

$$\Theta - \Theta_0 = T - T_0 + \Gamma z \qquad (5.10)$$

can be used to convert a temperature sounding (profile) into a potential temperature profile. The near-surface value Θ_0 can be calculated from Equation (5.7) if the surface pressure is known. A distinct advantage of using Equation (5.10) for calculating potential temperatures in the PBL is that one does not need to measure or estimate pressure at each height level.

The above relations are applicable to both dry and moist atmospheres, so long as water vapor does not condense and one uses the appropriate values of thermodynamic properties for the moist air. In practice, it is found to be more convenient to use constant dry-air properties such as R and c_p, but to modify some of the relations or variables for the moist air.

5.2.1 Moist unsaturated air

There are more than a dozen variables used by meteorologists that directly or indirectly express the moisture content of the air (Hess, 1959, Chapter 4). Of these the most often used in micrometeorology is the specific humidity (Q), defined as the ratio, $M_w/(M_w + M_d)$, of the mass of water vapor to the mass of moist air containing the water vapor. In magnitude, it does not differ significantly from the mixing ratio, defined as the ratio, M_w/M_d, of the mass of water vapor to the mass of dry air containing the vapor. Both are directly related to the water vapor pressure (e), which is the partial pressure exerted by water vapor and is a tiny fraction of the total pressure (P) anywhere in the PBL. To a good approximation,

$$Q \cong m_w e/m_d P = 0.622 e/P \qquad (5.11)$$

where m_w and m_d are the mean molecular masses of water vapor and dry air, respectively.

The water vapor pressure is always less than the saturation vapor pressure (e_s), which is related to the temperature through the Clausius–Clapeyron equation (Hess, 1959, Chapter 4)

$$\frac{de_s}{e_s} = \frac{m_w L_e}{R_*} \frac{dT}{T^2} \qquad (5.12)$$

where L_e is the latent heat of vaporization or condensation. Integration of Equation (5.12) and using the empirical fact (condition) that at $T = 273.2$ K,

$e_s = 6.11$ mbar, yields

$$\ln\frac{e_s}{6.11} = \frac{m_w L_e}{R_*}\left(\frac{1}{273.2} - \frac{1}{T}\right) \tag{5.13}$$

in which e_s is in millibars. A plot of e_s versus T is called the saturation water vapor pressure curve and is given in many meteorological textbooks and monographs.

Using Dalton's law of partial pressures ($P = P_d + e$), the equation of state for the moist air can be written as

$$P = \frac{R_*}{m}\rho T = \frac{R_*}{m_d}\frac{M_d}{V} T + \frac{R_*}{m_w}\frac{M_w}{V} T$$

or, after some algebra,

$$P = \frac{R_*}{m_d}\rho T\left[1 + \left(\frac{m_d}{m_w} - 1\right)Q\right] \tag{5.14}$$

After comparing Equation (5.14) to Equation (5.2) it becomes obvious that the factor in the brackets on the right-hand side of Equation (5.14) is the correction to be applied to the specific gas constant for dry air, R, in order to obtain the specific gas constant for the moist air. Instead of taking R as a humidity-dependent variable, in practice, the above correction is applied to the temperature in defining the virtual temperature

$$T_v = T\left[1 + \left(\frac{m_d}{m_w} - 1\right)Q\right] \cong T(1 + 0.61Q) \tag{5.15}$$

so that the equation of state for the moist air is given by

$$P = (R_*/m_d)\rho T_v = R\rho T_v \tag{5.16}$$

The virtual temperature is obviously the temperature which dry air would have if its pressure and density were equal to those of the moist air. Note that the virtual temperature is always greater than the actual temperature and the difference between the two, $T_v - T \cong 0.61QT$, may become as large as 7 K, which may occur over warm tropical oceans, and is usually less than 2 K over mid-latitude land surfaces.

For moist air one can define the virtual potential temperature, Θ_v, similar to that for dry air and use Equations (5.7) and (5.8) with Θ and T replaced by Θ_v and T_v, respectively.

The mixing ratio of water vapor in air being always very small (<0.04), the specific heat capacity is not significantly different from that of dry air. Therefore, changes in state variables of moving air parcels in an unsaturated atmosphere are not significantly different from those in a dry atmosphere, so long as the processes remain adiabatic. In particular, the adiabatic lapse rate given by Equation (5.4) is also applicable to most unsaturated air parcels moving in a moist environment, provided T in Equation (5.4) is replaced by T_v.

5.2.2 Saturated air

In saturated air, a part of the water vapor may condense and, consequently, the latent heat of condensation may be released. If condensation products (e.g., water droplets and ice crystals) remain suspended in an upward-moving parcel of saturated air, the saturated lapse rate, or the rate at which the saturated air cools as it expands with the increase in height, must be lower than the dry adiabatic lapse rate Γ, because of the addition of the latent heat of condensation in the former. If there is no exchange of heat between the parcel and the surrounding environment, such a process is called moist adiabatic.

From the first law of thermodynamics for the moist adiabatic process and the equation of state, the moist adiabatic or saturated lapse rate is given by (Hess, 1959):

$$\Gamma_s = -\left(\frac{\partial T}{\partial z}\right)_s = g\left(c_p + L_e \frac{dQ_s}{dT}\right)^{-1} \qquad (5.17)$$

where dQ_s/dT is the slope of the saturation-specific humidity versus temperature curve, as given by Equations (5.12) and (5.13). Unlike the dry adiabatic lapse rate, however, the saturated adiabatic lapse rate is quite sensitive to temperature. For example, at $T = 273.2$ K, $\Gamma_s = 0.0069$ K m^{-1} and at $T = 303$ K, $\Gamma_s = 0.0036$ K m^{-1}, both at the reference sea-level pressure of 1000 mbar.

In the real atmospheric situation, some of the condensation products are likely to fall out of an upward-moving parcel, while others may remain suspended as cloud particles in the parcel. As a result of these changes in mass and composition of the parcel, some exchange of heat with the surrounding air must occur. Therefore the processes within the parcel are not truly adiabatic, but are called pseudoadiabatic. The mass of condensation products being only a tiny fraction of the total mass of parcel, however, the pseudoadiabatic lapse rate is not much different from the moist adiabatic lapse rate.

The difference between the dry adiabatic and moist adiabatic lapse rates accounts for some interesting orographic phenomena, such as the formation of

clouds and possible precipitation on the upwind slopes of mountains and warm and dry downslope winds (e.g., Chinook and Foen winds) near the lee side base (Rosenberg *et al.*, 1983, Chapter 3).

Example Problem 1

A moist air parcel with a temperature of 20°C and specific humidity of 10 g kg^{-1} is lifted adiabatically from the upwind base of a mountain, where the pressure is 1000 mb, to its top, at 3000 m above the base, and is then brought down to the base on the other side of the mountain. Using the appropriate thermodynamic relations or diagrams, estimate the following parameters:

(a) The height z_s above the base where the air parcel would become saturated and the saturated adiabatic lapse rate at this level.
(b) The temperature of the parcel at the mountain top.
(c) The temperature of the parcel at the downwind base.

Solution

(a) First, we determine the temperature $T(z_s)$ at which the parcel would become saturated from Equation (5.13)

$$\ln\left(\frac{e_s}{6.11}\right) = 5404\left[\frac{1}{273.2} - \frac{1}{T(z_s)}\right]$$

where, from Equation (5.11),

$$e_s = Q_s P/0.622 \cong 0.0161 P(z_s)$$

The pressure and temperature of the parcel at the height z_s are related through the Poisson equation [Equation (5.6)] as

$$T(z_s) = T_0[P(z_s)/P_0]^{0.286}$$

The above expressions form a closed loop which can be solved, using an iterative procedure, to determine the variables at z_s as follows:

$$T(z_s) = 285.9 \text{ K}; \ P(z_s) = 917 \text{ mb}; \ e_s = 14.73 \text{ mb}$$

Then the height z_s is given by

$$z_s = (293.2 - 285.9)/0.0098 \cong 745 \text{ m}$$

Alternatively, z_s, $T(z_s)$, and $P(z_s)$ can also be determined from an appropriate thermodynamic diagram.

The saturated adiabatic lapse rate can be determined from Equation (5.17) in which

$$\frac{dQ_s}{dT} = 0.622 \frac{m_w L_e}{R_*} \frac{e_s}{PT^2} \cong 6.48 \times 10^{-4} \text{ K}^{-1}$$

Then,

$$\Gamma_s = 9.816/(1010 + 2.45 \times 648) \cong 0.0038 \text{ K m}^{-1}$$

(b) Assuming a constant saturated adiabatic lapse rate up to the top of the mountain at $z_t = 3000$ m, the temperature of the parcel there is given by

$$T(z_t) = T(z_s) - \Gamma_s(z_t - z_s) \cong 277.4 \text{ K}$$

However, this is only an approximation, because in reality dQ_s/dT is expected to vary with height. A more accurate estimate of the temperature at the mountain top can be obtained by following the moist adiabatic for $T = 286$ from the 745 m height level to 3000 m on a suitable thermodynamic diagram or chart.

(c) Assuming that the parcel remained unsaturated during its descent on the other side of the mountain, the temperature at the downwind base is given by

$$T_b = 277.4 + 0.0098 \times 3000 = 306.8 \text{ K}$$

which is 13.6 K higher than the air temperature at the upwind base.

This exercise shows that, in going up and down a high mountain, air temperature can increase substantially, provided that the lifting condensation level is well below the mountain top.

5.2.3 Thermodynamic energy equation

Using the principle of the conservation of energy within an elementary volume of air, one can derive the following differential equation for the variation of temperature (Kundu, 1990, Chapter 4):

$$\frac{DT}{Dt} = \alpha_h \nabla^2 T + S_H \tag{5.18}$$

where α_h is thermal diffusivity and S_H is the source term representing the rate of change of temperature within the elementary volume. Here, the total derivative DT/Dt represents the sum of the local change of temperature with time and advective changes in the same due to flow, while the ∇^2 (Laplacian) operator has the usual meaning. In deriving the simplified Equation (5.18), the so-called Boussinesq's approximations have been used and any change in temperature due to radiative flux divergence has been neglected. A similar equation can also be written for potential temperature.

5.3 Local and Nonlocal Concepts of Static Stability

The variations of temperature and humidity with height in the PBL lead to density stratification with the consequence that an upward- or downward-moving parcel of air will find itself in an environment whose density will, in general, differ from that of the parcel, after accounting for the adiabatic cooling or warming of the parcel. In the presence of gravity this density difference leads to the application of a buoyancy force on the parcel which would accelerate or decelerate its vertical movement. If the vertical motion of the parcel is enhanced, i.e., the parcel is accelerated farther away from its equilibrium position by the buoyancy force, the environment is called statically unstable. On the other hand, if the parcel is decelerated and is moved back to its equilibrium position, the atmosphere is called stable or stably stratified. When the atmosphere exerts no buoyancy force on the parcel at all, it is considered neutral. In general the buoyancy force or acceleration exerted on the parcel may vary with height and so does the static stability.

One can derive an expression for the buoyant acceleration, a_b, on a parcel of air by using the Archimedes principle and determining the net upward force due to buoyancy

$$a_b = g\left(\frac{\rho - \rho_p}{\rho_p}\right) \tag{5.19}$$

in which the subscript p refers to the parcel. Further, using the equation of state for the moist air, Equation (5.19) can also be written as

$$a_b = -g\left(\frac{T_v - T_{vp}}{T_v}\right) \tag{5.20}$$

5.3.1 Local static stability

Expressions (5.19) and (5.20) for the buoyant acceleration on a parcel in a
stratified environment are valid irrespective of the origin or initial position of
the parcel. An alternative, but approximate, expression for a_b in terms of the
local gradient of virtual temperature or potential temperature is often given in
the literature as

$$a_b \cong -\frac{g}{T_v}\left(\frac{\partial T_v}{\partial z} + \Gamma\right)\Delta z = -\frac{g}{T_v}\frac{\partial \Theta_v}{\partial z}\Delta z \tag{5.21}$$

This expression can be derived from Equation (5.20) by assuming that any
parcel displacement, Δz, from its equilibrium position is small and by expanding
T_v and T_{vp} in the Taylor series around their equilibrium value T_{ve}.

Equation (5.21) gives a criterion, as well as a quantitative measure, of static
stability of the atmosphere in terms of $\partial T_v/\partial z$ or $\partial \Theta_v/\partial z$. In particular, the static
stability parameter is defined as

$$s = (g/T_v)(\partial \Theta_v/\partial z) \tag{5.22}$$

Thus, qualitatively, the static stability is often divided into three broad
categories:

1. Unstable, when $s < 0$, $\partial \Theta_v/\partial z < 0$, or $\partial T_v/\partial z < -\Gamma$.
2. Neutral, when $s = 0$, $\partial \Theta_v/\partial z = 0$, or $\partial T_v/\partial z = -\Gamma$.
3. Stable, when $s > 0$, $\partial \Theta_v/\partial z > 0$, or $\partial T_v/\partial z > -\Gamma$.

The magnitude of s provides a quantitative measure of static stability. It is quite
obvious from Equation (5.21) that vertical movements of parcels up or down
are generally enhanced in an unstable atmosphere, while they are suppressed in
a stably stratified environment. Note that, for an upward-moving parcel, $a_b > 0$
in a statically unstable environment and $a_b < 0$ in a stable environment.

On the basis of virtual temperature gradient or lapse rate (LR), relative to the
adiabatic lapse rate Γ, atmospheric layers are variously characterized as follows:

1. Superadiabatic, when $LR > \Gamma$.
2. Adiabatic, when $LR = \Gamma$.
3. Subadiabatic, when $0 < LR < \Gamma$.
4. Isothermal, when $\partial T_v/\partial z = 0$.
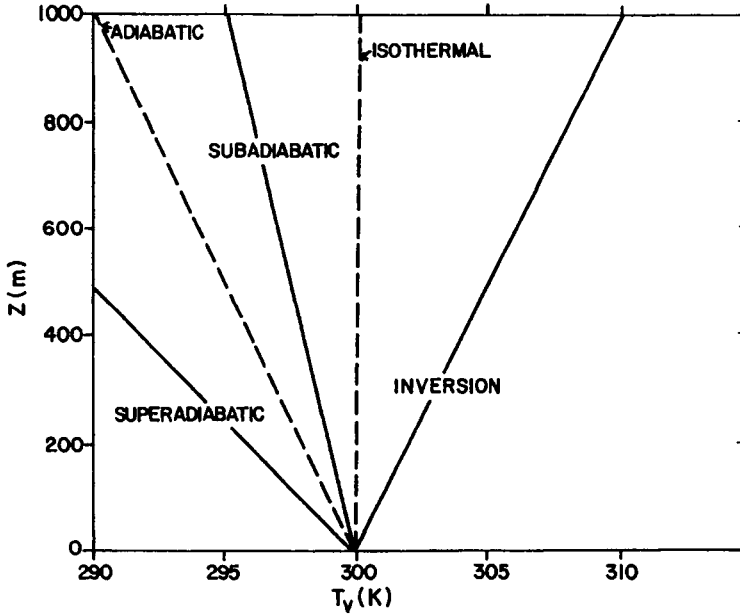5. Inversion, when $\partial T_v/\partial z > 0$.

Figure 5.1 Schematic of the various stability categories on the basis of virtual temperature gradient.

Figure 5.1 gives a schematic of these static stability categories in the lower part of the PBL. Here, the surface temperature is assumed to be the same and virtual temperature profiles are assumed to be linear for convenience only; actual profiles are usually curvilinear, as will be shown later.

This traditional view of static stability, based on the local gradient of virtual temperature or potential temperature has some serious limitations and is not very satisfactory, especially when static stability is used as a measure of turbulent mixing and diffusion. For example, it is well known that in the bulk of the convective boundary layer (CBL), $\partial\Theta_v/\partial z \cong 0$, or is slightly positive. Its characterization as a neutral or slightly stable layer, according to the traditional definition of static stability based on the local gradient, would be very misleading because the convective mixed layer (the middle part of the CBL where $\partial\Theta_v/\partial z \cong 0$) has all the attributes of an unstable boundary layer, such as upward heat flux, vigorous mixing, and large thickness. It would be correctly recognized as an unstable layer if one considers the positive buoyancy forces or accelerations that would act in all the warm air parcels originating in the superadiabatic layer near the surface. For these parcels, experiencing large displacements, before they arrive in the mixed layer, Equation (5.21) is not valid and the local static stability parameter becomes irrelevant. Thus, s is not a good

measure of buoyant accelerations or forces on air parcels undergoing large displacements from their equilibrium positions. The differences in densities or virtual temperatures between parcels and the environment are the simplest and most direct measures of buoyancy forces and should be considered in any stability characterization of the environment. The original criterion for determining static stability in terms of buoyancy forces on parcels coming from all possible initial positions appears to be basically sound. It is only when one considers the alternative criterion in terms of the local lapse rate, $\partial \Theta_v / \partial z$, or s that ambiguities arise in certain situations.

5.3.2 Nonlocal static stability

In order to remove the ambiguities associated with the concept of local static stability, Stull (1988, Chapter 5; 1991) has proposed a nonlocal characterization of stability. For this, an environmental sounding of thermodynamic variables should be taken over a deep layer between the surface and the level where vertical parcel movements are likely to become insignificant (e.g., strong inversion or the tropopause). To determine the stability of the various layers, air parcels should be displaced up and down from all possible starting points within the whole domain. In practice, one needs to consider parcels starting from only the relative minima and maxima of the virtual potential temperature sounding or profile. Air parcel movement up or down from the initial position should be based on the parcel buoyancy and not on the local lapse rate. The parcel buoyancy at any level is determined by the difference in virtual temperatures of the parcel and the environment at that level. Buoyancy forces warm air parcels to rise and cold parcels to sink. Displaced air parcels that would continue to move farther away from their starting level should be tracked all the way to the level where they would become neutrally buoyant ($T_{vp} = T_v$, or $\Theta_{vp} = \Theta_v$). After parcel movements from all the salient levels (minima and maxima in the Θ_v profile) have been tracked, nonlocal static stability of different portions (layers) of the sounding domain should be determined in the following order (Stull, 1991):

1. *Unstable*: Those regions in which parcels can enter and transit under their own buoyancy. Individual air parcels need not traverse the whole unstable region. Many parcels would traverse only a part of the unstable region or layer.
2. *Stable*: Those regions of subadiabatic lapse rate that are not unstable.
3. *Neutral*: Those regions of adiabatic lapse rate that are not unstable.
4. *Unknown*: Those top or bottom portions of the sounding that are apparently stable or neutral, but that do not end at a material surface, such as the

ground surface, strong inversion, or the tropopause. Above or below the known sounding region might be a cold or warm layer, respectively, that could provide a source of buoyant air parcels.

The above method or procedure for determining the nonlocal stability is illustrated in Figure 5.2 for the various hypothetical, but practically feasible, soundings (Θ_v profiles). Note that in some of these cases, especially those with unstable regions, the traditional characterizations of stability based on the local lapse rate or $\partial\Theta_v/\partial z$ would be quite different from the broader, nonlocal characterization used here. The latter are based on the buoyant movements (indicated by vertical dashed lines and arrows in Figure 5.2) of air parcels, some of which are undergoing large displacements.

When compared with traditional local static stability measures, the nonlocal characterization of stability is more consistent with the empirical evidence that unstable and convective boundary layers have strong and efficient mixing, while the stable boundary layer and other inversion layers have relatively weak mixing associated with them. The former is recommended as the preferred choice for
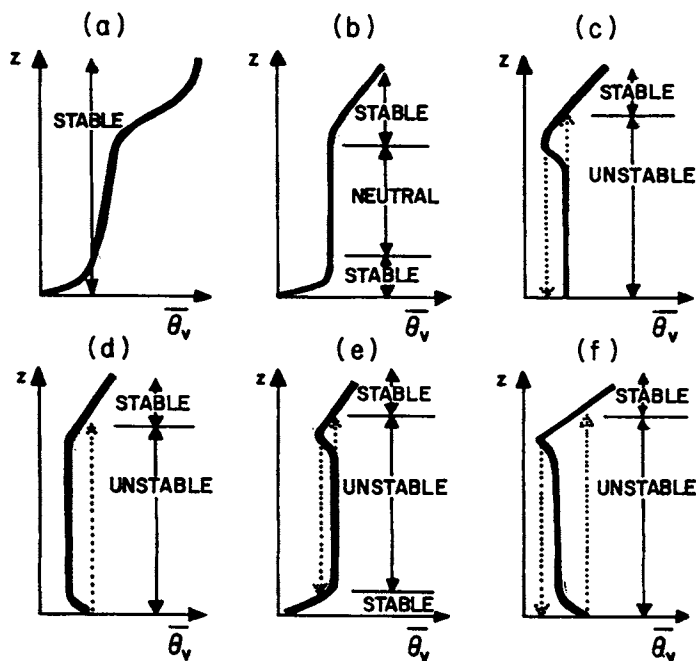

Figure 5.2 Nonlocal stability characterization for the various hypothetical virtual potential temperature profiles. [After Stull (1988).]

applications in micrometeorology and air pollution meteorology (Arya, 1999, Chapter 2).

Example Problem 2
The following measurements were made from the research vessel FLIP during the 1969 Barbados Oceanographic and Meteorological Experiment (BOMEX):

Height above sea-surface (m):	2.1	3.6	6.4	11.4
Air temperature (°C):	27.74	27.72	27.69	27.62
Specific humidity (g kg^{-1}):	18.02	17.83	17.54	17.29

(a) Calculate the virtual temperature at each level and its difference from the actual temperature.
(b) Calculate and compare the gradients of potential temperature and virtual potential temperature between adjacent measurement levels.
(c) Calculate the local static stability parameter, s, and the percentage contribution of specific humidity gradient to the same at different height levels.

Solution
(a) Using $T_v = T(1 + 0.61Q)$ and $T_v - T = 0.61QT$, where T and T_v are in absolute units (K) and Q is dimensionless, we obtain the following:

z (m):	2.1	3.6	6.4	11.4
T_v (K):	304.25	304.19	304.11	303.99
$(T_v - T)$ (K):	3.31	3.21	3.22	3.17

(b) Estimating the gradients between adjacent levels as

$$\frac{\partial T}{\partial z} \cong \frac{\Delta T}{\Delta z}; \quad \frac{\partial T_v}{\partial z} \cong \frac{\Delta T_v}{\Delta z}$$

and using the approximate relations

$$\frac{\partial \Theta}{\partial z} \cong \frac{\partial T}{\partial z} + \Gamma; \quad \frac{\partial \Theta_v}{\partial z} \cong \frac{\partial T_v}{\partial z} + \Gamma$$

We can estimate and compare the above gradients as follows:

Mean height (m):	2.85	5.00	8.90
$\partial \Theta/\partial z$ (K m^{-1}):	−0.0035	−0.0009	−0.0042
$\partial \Theta_v/\partial z$ (K m^{-1}):	−0.0302	−0.0188	−0.0142

Note that magnitudes of $\partial \Theta_v / \partial z$ over the tropical ocean are much larger than those of $\partial \Theta / \partial z$.

(c) Using the definition

$$s = \frac{g}{T_v} \frac{\partial \Theta_v}{\partial z},$$

it can easily be calculated. For determining the relative contribution of the specific humidity gradient to s, we can write

$$s = \frac{g}{T_v} \left(\frac{\partial T_v}{\partial z} + \Gamma \right) = \frac{g}{T_v} \left(\frac{\partial T}{\partial z} + 0.61 T \frac{\partial Q}{\partial z} + \Gamma \right)$$

$$= \frac{g}{T_v} \left(\frac{\partial \Theta}{\partial z} + 0.61 T \frac{\partial Q}{\partial z} \right)$$

The second term represents the contribution of the specific humidity gradient to s. The relative contribution of the same is given by

$$0.61 T \frac{\partial Q}{\partial z} \bigg/ \frac{\partial \Theta_v}{\partial z} = 1 - \frac{\partial \Theta / \partial z}{\partial \Theta_v / \partial z}$$

Mean height (m):	2.85	5.00	8.90
Static stability (s^{-2}):	-9.74×10^{-4}	-6.02×10^{-4}	-4.54×10^{-4}
% contribution of $\partial Q / \partial z$:	88.4	95.2	70.4

This example illustrates that it is extremely important to include the specific humidity gradients in any estimates of static stability over water surfaces. The stability based on temperature alone would be characterized as near-neutral, while it is significantly unstable, because of the stronger negative humidity gradients.

5.4 Mixed Layers, Mixing Layers and Inversions

In moderate to extremely unstable conditions, typically encountered during midday and afternoon periods over land, mixing within the bulk of the boundary layer is intense enough to cause conservable scalars, such as Θ and Θ_v, to be distributed uniformly, independent of height. The layer over which this occurs is called the mixed layer, which is an adiabatic layer overlying a superadiabatic surface layer. To a lesser extent, the specific humidity, momentum, and concentrations of pollutants from distant sources also have uniform

distributions in the mixed layer. Mixed layers are found to occur most persistently over the tropical and subtropical oceans.

Sometimes, the term 'mixing layer' is used to designate a layer of the atmosphere in which there is significant mixing, even though the conservable properties may not be uniformly mixed. In this sense, the turbulent PBL is also a mixing layer, a large part of which may become well mixed (mixed layer) during unstable conditions. Mixing layers are also found to occur sporadically or intermittently in the free atmosphere above the PBL, whenever there are suitable conditions for the breaking of internal gravity waves and the generation of turbulence in an otherwise smooth, streamlined flow.

The term 'inversion' in common usage applies to an atmospheric condition when air temperature increases with height. Micrometeorologists sometimes refer to inversion as any stable atmospheric layer in which potential temperature (more appropriately, Θ_v) increases with height. The strength of inversion is expressed in terms of the layer-averaged $\partial \Theta_v / \partial z$ or the difference $\Delta \Theta_v$ across the given depth of the inversion layer.

Inversion layers are variously classified by meteorologists according to their location (e.g., surface and elevated inversions), the time (e.g., nocturnal inversion), and the mechanism of formation (e.g., radiation, evaporation, advection, subsidence, frontal and sea-breeze inversions). Because vertical motion and mixing are considerably inhibited in inversions, a knowledge of the frequency of occurrence of inversions and their physical characteristics (e.g., location, depth, and strength of inversion) is very important to air pollution meteorologists. Pollutants released within an inversion layer often travel long distances without much mixing and spreading. These are then fumigated to ground level as soon as the inversion breaks up to the level of the ribbonlike thin plume, resulting in large ground-level concentrations. Low-level and ground inversions act as lids, preventing the downward diffusion or spread of pollutants from elevated sources. Similarly, elevated inversions put an effective cap on the upward spreading of pollutants from low-level sources. An inversion layer usually caps the daytime unstable or convective boundary layer, confining the pollutants largely to the PBL. Consequently, the PBL depth is commonly referred to as the mixing depth in the air quality literature.

The most persistent and strongest surface inversions are found to occur over the Antarctica and Arctic regions; the tradewind inversions are probably the most persistent elevated inversions capping the PBL.

5.5 Vertical Temperature and Humidity Profiles

A typical sequence of observed potential temperature profiles at 3 h intervals during the course of a day is shown in Figure 5.3. These were obtained from
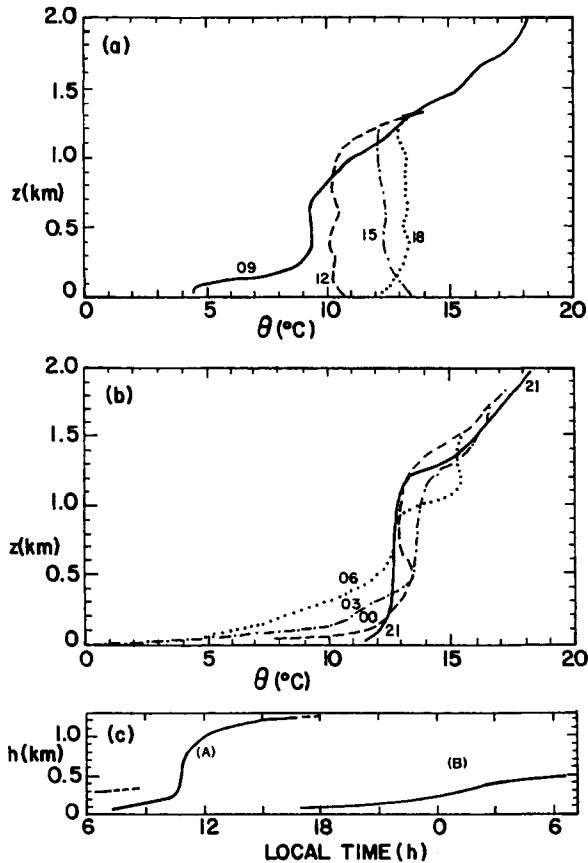
Figure 5.3 Diurnal variations of potential temperature profiles and inversion heights during (a) day 33 and (b) days 33–34 of the Wangara Experiment. (c) Curve A, inversion base height in the daytime CBL. Curve B, surface inversion height in the nighttime SBL. [After Deardorff (1978).]

radiosonde measurements during the 1967 Wangara Experiment near Hay, New South Wales, Australia, on a day when there were clear skies, very little horizontal advections of heat and moisture, and no frontal activity within 1000 km.

Note that, before sunrise and at the time of the minimum in the near-surface temperature, the Θ profile is characterized by nocturnal inversion, which is produced as a result of radiative cooling of the surface. The nocturnal boundary layer is stably stratified, so that vertical turbulent exchanges are greatly suppressed. It is generally referred to as the stable boundary layer (SBL). Shortly after sunrise, surface heating leads to an upward exchange of sensible

heat and subsequent warming of the lowest layer due to heat flux convergence. This process progressively erodes the nocturnal inversion from below and replaces it with an unstable or convective boundary layer (CBL) whose depth h grows with time (see Figure 5.3c). The rate of growth of h usually attains maximum a few hours after sunrise when all the surface-based inversion has been eroded, and slows down considerably in the late afternoon.

The daytime unstable or convective boundary layer has a three-layered structure. The potential temperature decreases with height within the shallow surface layer. In this layer, turbulence is generated by both wind shear and buoyancy. The surface layer is followed by the mixed layer in which potential temperature remains more or less uniform. The mixed layer comprises the bulk of the CBL. This layer is dominated by buoyancy-generated turbulence, except during morning and evening transition hours when shear effects also become important. Above the mixed layer is a shallow transition layer in which potential temperature increases with height. In this stable layer, turbulence decreases rapidly with height. From the temperature sounding alone, the top of the PBL, including the transition layer, is not as distinct as the top of the mixed layer which is also the base of the inversion. Therefore, the height of inversion (z_i) is often used as an approximation for the PBL height (h), although the former can be substantially (10–30%) smaller than the latter.

Just before sunset, there is net radiative loss of energy from the surface and, consequently, an inversion forms at the surface. The nocturnal inversion deepens in the early evening hours and sometimes throughout the night, as a result of a radiative and sensible heat flux divergence. The surface inversion height (h_i) may not correspond to the height, h, of the stable boundary layer (SBL) based on significant turbulence activity. The inversion height is more easily detected from temperature soundings and is depicted in Figure 5.3c. The PBL height can be directly measured from remote-sensing instruments such as sodar and lidar or indirectly estimated from both temperature and wind profiles. Such measurements indicate that, unlike the surface inversion height, the PBL height (h) generally decreases with time during early evening hours and attains a constant value which is usually less than h_i. Sometimes, the PBL height oscillates around some average value throughout the night.

The SBL is often capped by the remnant of the previous afternoon's mixed layer. Mixing processes in this so-called residual layer are likely to be very weak. Strong wind shears may generate some intermittent and sporadic turbulence, which is not connected to the SBL.

Observed vertical profiles of specific humidity for the same Wangara day 33 are shown in Figure 5.4. The surface during this period of drought was rather dry, with little or no growth of vegetation (predominantly dry grass, legume, and cottonbush). In the absence of any significant evapotranspiration from the surface, the specific humidity profiles are nearly uniform in the daytime PBL,
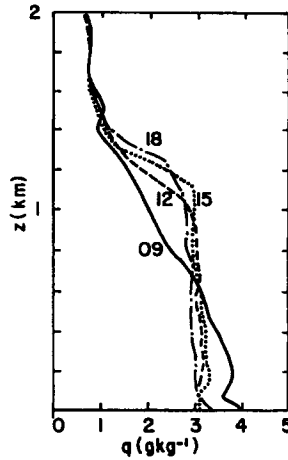
Figure 5.4 Diurnal variation of specific humidity profiles during day 33 of the Wangara Experiment. [From Andre *et al.* (1978).]

with the value of Q changing largely in response to the evolution of the mixed layer.

In other situations where there is dry air aloft, but plenty of moisture available for evaporation at the surface, the evolution of Q profiles might be quite different from those shown in Figure 5.4. In response to the increase in the rate of evaporation or evapotranspiration during the morning and early afternoon hours, Q may actually increase and attain its maximum value sometime in the afternoon and, then, decrease thereafter, as the evaporation rate decreases.

The evaporation from the surface, although strongest by day, may continue at a reduced rate throughout the night. Under certain conditions, when winds are light and the surface temperature falls below the dew point temperature of the moist air near the surface, the water vapor is likely to condense and deposit on the surface in the form of dew. The resulting inversion in the Q profile leads to a downward flux of water vapor and further deposition.

Temperature and humidity profiles over open oceans do not show any significant diurnal variation when large-scale weather conditions remain unchanged, because the sea-surface temperature changes very little (typically, less than 0.5°C), if at all, between day and night. Figure 5.5 shows the observed profiles of T and Q from two research vessels (with a separation distance of about 750 km) during the 1969 Atlantic Tradewind Experiment (ATEX). Here, only the averaged profiles for the two periods designated as 'undisturbed' (February 7–12) and 'disturbed' (February 13–17) weather are given. During the undisturbed period, the temperature and humidity structure of the PBL is characterized by a mixed layer (depth $\cong 600$ m), followed by a shallow
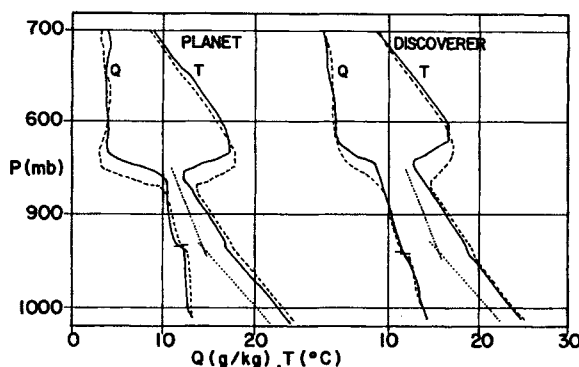
Figure 5.5 Observed mean vertical profiles of temperature and specific humidity at two research vessels during ATEX. First ('undisturbed') period: solid lines; second ('disturbed') period: dashed lines. The dotted lines indicate the dry adiabatic and saturated adiabatic lapse rates. [After Augstein *et al.* Copyright © (1974) by D. Reidel Publishing Company. Reprinted by permission.]

isothermal transition layer (depth $\cong$ 50 m) and a deep cloud layer extending to the base of the trade wind inversion. The same features can also be seen during the disturbed period, but with larger spatial differences.

At the other extreme, Figure 5.6 shows the measured mean temperature profiles in the surface inversion layer at the Plateau Station, Antarctica (79°15'S, 40°30'E), in three different seasons (periods) and for different stability classes (identified here as (1) through (8) in the order of increasing stability and defined from both the temperature and wind data). These include some of the most stable conditions ever observed on the earth's surface.

5.6 Diurnal Variations

As a result of the diurnal variations of net radiation and other energy fluxes at the surface, there are large diurnal variations in air temperature and specific humidity in the PBL over land surfaces. The diurnal variations of the same over large lakes and oceans are much smaller and often negligible.

The largest diurnal changes in air temperature are experienced over desert areas where strong large-scale subsidence limits the growth of the PBL and the air is rapidly heated during the daytime and is rapidly cooled at night. The mean diurnal range of screen-height temperatures is typically 20°C, with mean maximum temperatures of about 45°C during the summer months (Deacon, 1969).
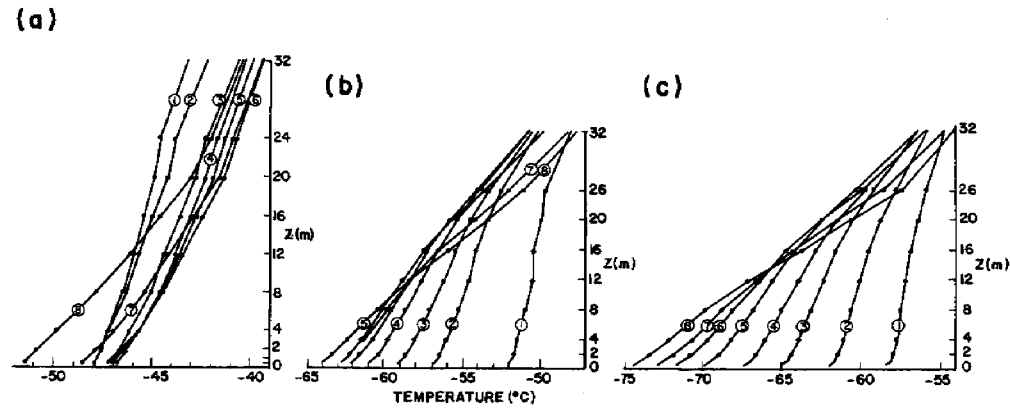
Figure 5.6 Observed mean temperature profiles in the surface inversion layer at Plateau Station, Antarctica, for three different periods grouped under different stability classes. (a) Sunlight periods, 1967; (b) transitional periods, 1967; (c) dark season, 1967. [After Lettau *et al.* (1977).]

The diurnal range of temperatures is reduced by the presence of vegetation and the availability of moisture for evaporation. Even more dramatic reductions occur in the presence of cloud cover, smoke, haze, and strong winds. The diurnal range of temperatures decreases rapidly with height in the PBL and virtually disappears at the maximum height of the PBL or inversion base, which is reached in the late afternoon. Some examples of observed diurnal variations of air temperature at different heights and under different cloud covers and wind conditions are given in Figure 5.7.
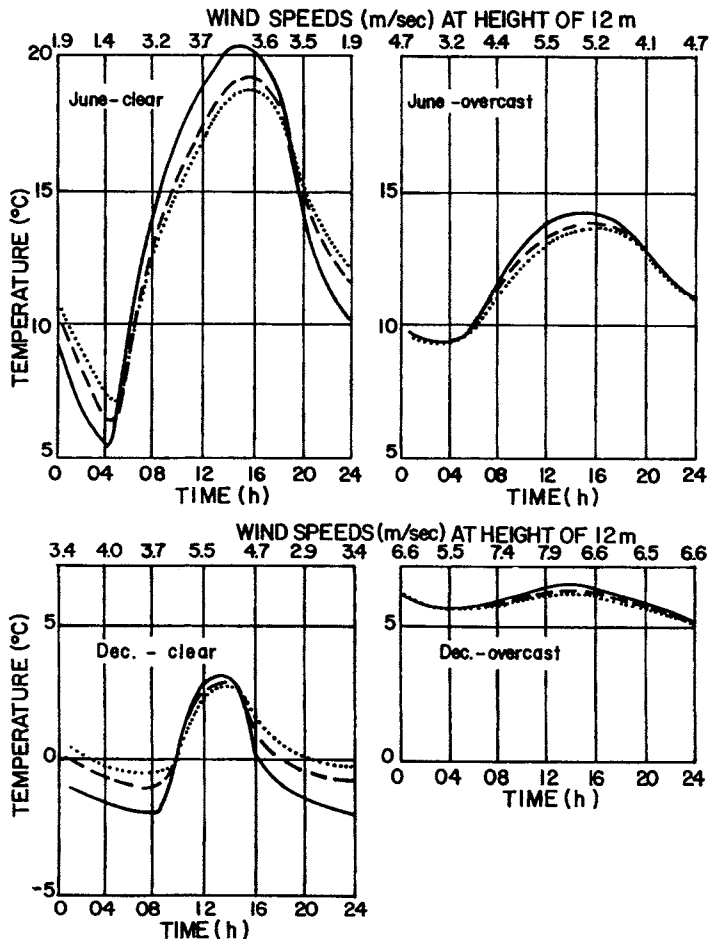

Figure 5.7 Diurnal variation of air temperature at three heights (solid lines: 1.2 m; dashed lines: 7 m; dotted lines: 17 m) over downland in Southern England for various combinations of clear and overcast days in June and December. Wind speeds at 12 m height are also indicated. [From Deacon (1969); after Johnson (1929).]
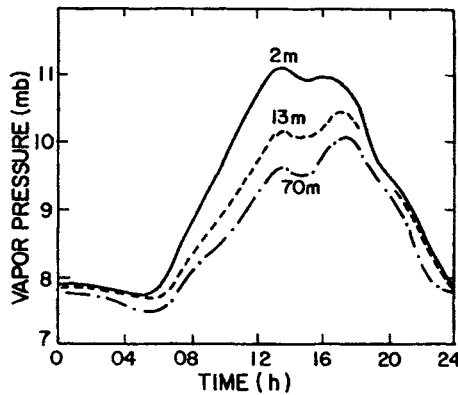
Figure 5.8 Diurnal variation of water vapor pressure at three heights at Quickborn, Germany, on clear May days. [From Deacon (1969).]

The diurnal variation of specific humidity depends on the diurnal course of evapotranspiration and condensation, surface temperatures, mean winds, turbulence, and the PBL height. Large diurnal changes in surface temperature generally lead to large variations of specific humidity, due to the intimate relationship between the saturation vapor pressure and temperature. Figure 5.8 illustrates the diurnal course of water vapor pressure at three different heights. Here the secondary minimum of vapor pressure in the afternoon is believed to be caused by further deepening of the mixed layer after evapotranspiration has reached its maximum value. This phenomenon may be even more marked at other places and times.

5.7 Applications

The knowledge of air temperature and humidity in the PBL is useful and may have applications in the following areas:

- Determining the static stability of the lower atmosphere and identifying mixed layers and inversions.
- Determining the PBL height, as well as the depth and strength of surface or elevated inversion.
- Predicting air temperature and humidity near the ground and possible fog and frost conditions.
- Determining the sensible heat flux and the rate of evaporation from the surface.
- Calculating atmospheric radiation.

- Estimating diffusion of pollutants from surface and elevated sources and possible fumigation.
- Designing heating and air-conditioning systems.

Problems and Exercises

1. How do the mechanisms of heat transfer in the atmosphere differ from those in a subsurface medium, such as soil and rock?

2.
(a) Derive the following equation for the variation of air temperature with time, in the absence of any horizontal and vertical advections of heat:

$$\rho c_p (\partial T/\partial t) = (\partial R_N/\partial z) - (\partial H/\partial z)$$

(b) Indicate how the above equation may be used to estimate the sensible heat flux at the surface, H_0, during the daytime when the rate of warming is nearly constant through the depth of the PBL.
(c) Temperature measurements at the top of a 20 m tower indicated a rate of warming of 1.8 °C h^{-1} during the mid-day period when the PBL height was estimated to be 850 m from a minisonde sounding. Estimate the surface heat flux at the time of observations.

3.
(a) Derive an expression for the adiabatic lapse rate in a moist, unsaturated atmosphere and discuss the effect of moisture on the same.
(b) Explain why the saturated adiabatic lapse rate must be smaller than the dry diabatic lapse rate.

4.
(a) Derive the equation of state for the moist air and hence define the virtual temperature T_v.
(b) Show that, to a good approximation,

$$\partial T_v/\partial z = (\partial T/\partial z) + 0.61T(\partial Q/\partial z)$$

5.
(a) Show that the buoyant acceleration on a parcel of air in a thermally stratified environment is given by

$$a_b = -(g/T_v)(T_v - T_{vp})$$

(b) Considering a small vertical displacement, Δz, from the equilibrium position of the parcel, show that

$$a_b \cong -(g/T_v)(\partial\Theta_v/\partial z)\Delta z$$

6. A moist air parcel at a temperature of 30°C and specific humidity of 25 g kg^{-1} is lifted adiabatically from the upwind base of a tropical mountain island, where the pressure is 1000 mb, to the top, at 2000 m above the base, and is then brought down to the base on the other side of the mountain. Using appropriate equations or tables, calculate the following parameters:
(a) The height above the base where the air parcel would become saturated and the saturated adiabatic lapse rate at this level.
(b) The temperature of the parcel at the top of the mountain.
(c) The temperature of the parcel at the downwind base, assuming that the parcel remained unsaturated during its entire descent.

7. The following pressure, temperature and specific humidity measurements were made from radiosonde soundings on day 11 of the Wangara PBL experiment:

Height (m)	Pressure (mb)	Temperature (°C)	Specific humidity (g kg^{-1})
Surface (1.5)	1013	11.8	6.5
50	1007	10.9	6.1
100	1001	10.1	5.8
150	995	9.6	5.6
200	989	9.2	5.5
300	977	8.4	5.3
400	965	7.4	5.1
500	954	6.4	4.9
550	948	6.0	4.9
600	942	5.6	4.8
650	936	5.1	4.7
700	931	4.9	4.6
750	925	4.9	4.5
800	919	4.9	4.5
850	914	5.0	4.5
900	908	5.0	4.5
1000	897	4.8	4.4

(a) Calculate and plot virtual temperature as a function of height.
(b) Calculate and plot virtual potential temperature as a function of height.

(c) Characterize the various layers on the basis of local and nonlocal stability and discuss the differences between the two.
(d) Estimate the height of the inversion base (z_i), as well as the PBL height (h). Discuss the sensitivity of the latter to the near-surface temperature.

8. Discuss the importance of specific humidity gradient in the determination of the static stability parameter s over different types of surfaces. Under what conditions can one ignore specific humidity in the determination of static stability?